

# Model of the Connector for 3D Distance Knitted Fabric Fastened by Articulated Joints

## Abstract

During the first stage of our considerations, a model of the compression process of a 3D distance knitted fabric was related to a single connector fastened to it by articulated joints, and considered as a slender rod with an assumed shape. In our physical and mathematical models, the compression of a slender, elastic rod was based on assumptions concerning the knitted fabric's morphology, as well as the mechanical properties of the threads, particularly monofilaments placed in the internal layer of the fabric. A calculation method was developed which enables to determine the functional dependencies between the compressing force and bending deflection, as well as a method of determining curves representing the shape of the compressed rod – connector. A computer simulation of the compressed rod connecting the two outside layers of the knitted fabric, considering the variable parameters of the model, was carried out with the use of calculation algorithms elaborated by us, and MathCad program.

**Key words:** knitted 3D fabric, distance fabric, compression process, connector, articulated joint, mathematical model, physical model, simulation.

## Introduction

The modelling was carried out with the aim of finding the optimum procedure which would facilitate in solving the problem of 3D distance knitted fabric compression. The process of compressing such a fabric is accompanied by a number of physical, particularly mechanical phenomena, such as the bending of the connectors, which form the knitted fabric's structure, and the mutual interaction of the friction between neighbouring connectors, among others. Designing a distance knitted fabric which would fulfil the demands of its future user is a complex procedure. Irrespective of the shape of such a fabric, described by its geometry, it should fulfil a number of usability requirements, including sufficient, mainly high strength, and resistance to the action of external forces. An analysis of literature carried out by us concerning the structure and mechanical properties of 3D knitted fabrics and the modelling of their strength behaviour led to the conclusion that the problems of modelling the compression of such fabrics have hitherto not been described. Therefore, developing a model description of the fabric's compression process will create the possibility of designing distance fabrics of assumed elasticity without the need to manufacture a prototype. The designing process concerning geometric and technological aspects will be completed by selecting an appropriate material, and next manufacturing the fabric with the use of a suitable knitting machine without the need to carry out

initial experimental stages. Such a procedure will allow to significantly shorten the designing time of 3D distance knitted fabric.

## Assumptions of the model

The object compressed, which is a 3D distance knitted fabric, is considered as two rigid planes connected by a network of rods which form an elastic spatial trust. The shape of this trust depends on the knitted structure of the stitches, as well as on the mechanical properties of the threads which form the structure [1]. Modelling the compression process of the knitted fabric was performed during the first stage of the investigation, assuming a single connector comprising a rod joining the outside layers of the knitted fabric.

The rod compressed we considered as placed in the xyz co-ordinate system, and to facilitate the analysis of the phenomenon, we mentally divided the rod – connector into two rods consisting of its projections on the perpendicular planes 0xz and 0xy, which are the planes of two cross-sections of the knitted fabric (*Figure 1*).

The outside planes,  $p_1$  and  $p_2$ , of the knitted fabric are composed of single loops or loops connected into loop systems. The loops consist of single systems of the outside planes  $p_1$  and  $p_2$ . We consider them as basic elements of the planes' structure with a dimension of  $A \times B$ , where  $B$  is the width of the wale, and  $B$  is the height of the course. The segments do not deform, which means that  $A = \text{constant}$  and  $B = \text{constant}$ . The loops of the model

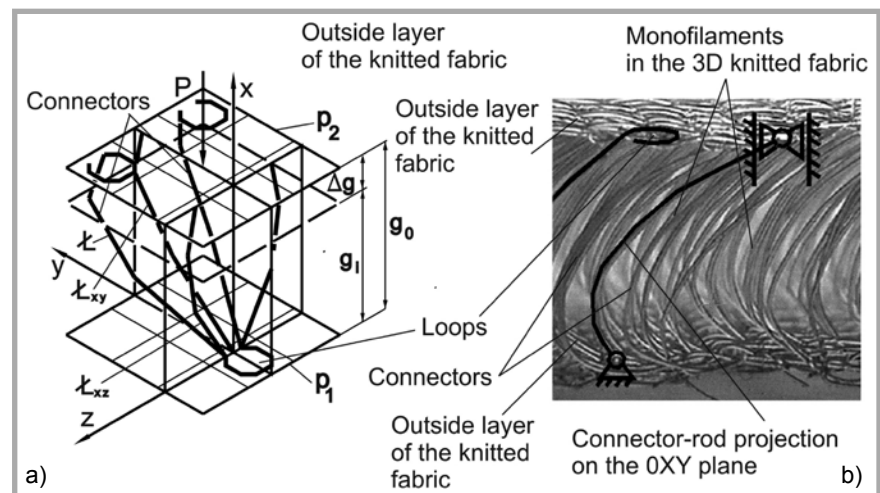


**Figure 1.** 3D distance knitted fabric; a) design of the fabric, b) photograph of the cross-section of a 3D distance knitted fabric.

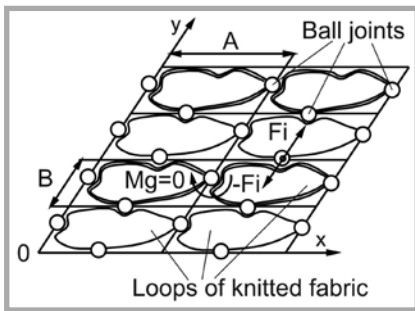


Figure 2. Physical model of the outside planes of the 3D knitted fabric.

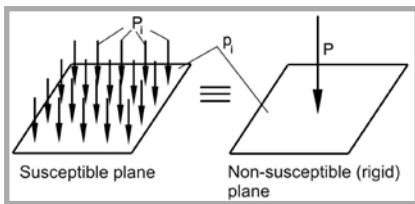


Figure 3. Equivalent load of the planes of the 3D distance knitted fabric.

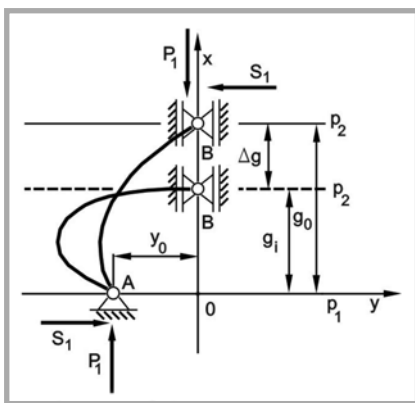


Figure 4. Fastening scheme of the physical object – a bent elastic rod.

planes are connected by articulated ball joints (Figure 2).

From a mechanical point of view, we consider the planes as shells which are susceptible to deflection and non-susceptible to stretching. For such a model of the planes  $p_1$  and  $p_2$  accepted by us, only small and insignificant bending moments occur ( $M_g \cong 0$ ) at the points of loop joints. Only the mutual influence of neighbouring elements, e.g. of loops, occurs due to the reaction forces ( $F_i$ ) in the articulated joints, which act on the surface of the shell.

In the case of the compression process of 3D distance knitted fabric, in order to accept a uniformly distributed load caused by the unit forces  $P_i$  acting on the singular loop segments, we assume that this is equivalent to the impact of a singular

force  $P$  acting at the midpoint of the surface of the rigid plane  $p_1$  (Figure 3).

The following dependency connects the unit forces  $P_i$  with the summary force  $P$ :

$$P = \sum \cdot P_i$$

where:  $m$  – is the number of loops closed by the surface of plane  $p_1$ .

The structural model of the plane accepted by us may be related to the process of compressing the distance knitted fabric with the use of a tensile tester. In this case, the rigid dished disks connected to the measuring head of a tensile tester perform the compression process of the sample investigated.

The physical model of compressing a slender, elastic rod in a single plane,  $Oxz$  or  $Oxy$ , is based on the following assumptions:

- the planes of the knitted fabric are displaced in the transversal direction,
- the loading by force  $P$  acts in a direction perpendicular to the planes of the knitted fabric,
- the connectors are considered as elastic rods whose structure has a spatial configuration, as well as elements fastened by an articulated joint to the outside surfaces of the knitted fabric at both ends,
- the connectors which belong to a single loop are joined at a single point, the planes  $p_1$  and  $p_2$  are not deformed (this is a simplifying assumption of our analysis, as the connector considered presents a whole set of connectors the fact that the knitted distance fabric analysed). In the event that such an assumption would not be accepted, irrespective of all the connector loads acting are of the same value, the connectors would be characterised by different deflections, which in turn would complicate the considerations. An analysis taking into account loads causing irregular connector deflections will be the subject of our future works and publications;
- in the preliminary stage of the compression process, the rods retain the assumed shape, and next, with an increasing force  $P_1$ , a transversal force  $S_1$  of the base reaction appears,
- such factors as temperature and humidity do not influence the proceeding of the deformation process of the knitted fabric.

In a further analysis of the mathematical model based on the physical model, the

connector is considered as a slender rod with an assumed shape, which is affected by the bending process. The assumed shape is obtained by accepting the thickness  $g_0$  of the knitted fabric at which the deflection value  $\Delta g$  takes the zero value, and the mutual displacement  $y_0$  of the rod's end in the direction perpendicular to the deflection, as well as the assumed length  $l_p$  of the rod. The rod is considered in a free state (not loaded) and takes such a shape that its potential energy will be the smallest.

### Physical model of the compression process

Taking into consideration all aspects related to the structure of the 3D distance knitted fabric, as well as the behaviour of this fabric under the influence of loads acting on the fabric, and on the basis of the assumptions mentioned in the previous chapter, below is presented a physical model of a slender, elastic rod of assumed shape. The general assumption is that the rods are fastened at both ends by articulated joints.

As far as compressed rods are concerned, the model discussed is related to the Euler's theory, the difference being that our assumption, confirmed empirically, considers the rod as a slender object with assumed preliminary shape; what connects is existing of additional forces  $S_1$  that occur during the compression process, which are caused by the reaction of the base i.e., the reaction of the outside layers of the knitted fabric [2-5]. Figure 4 presents a scheme of the mechanical model in the form of a rod mentally liberated from constraints; this presents the outside planes of the knitted fabric, whose action was substituted by the forces  $P_1$  and  $S_1$ , and their motion is limited by both the immovable and slidable articulated joints. The following designations are marked in Figure 4:

- $g_0$  – initial thickness of the knitted fabric,
- $g_i$  – thickness of the fabric during compression,
- $\Delta g$  – deflection of the knitted fabric,
- $p_1, p_2$  – planes in which the knitted fabric's loops are placed,
- $y_0$  – horizontal displacement of the rod's fastening points,
- $P_1$  – force compressing the bent rod, and
- $S_1$  – transversal force of the base's reaction.

## Mathematical model of the compression process of a single connector

The physical model presented above enables to formulate parametrical, functional as well as normal differential equations of the fourth order, which interrelate the load of the rod with its deformations. The rod-connector is considered and accepted by us as two individual rods which are the projections of the rod on the 0xz and 0yz planes.

The differential equation which describes deformations of the rod influenced by the load has the following form:

$$EJy''(x) = -P_1y'(x) + S_1x \quad (1)$$

where  $y(x) = y_0(x) + y_1(x)$

where:

$y_0(x)$ , and  $y_1(x)$  are the initial buckling, and the buckling occurring as result of the force  $P_1$  action, respectively;

$S_1$  – is the reaction force of the transversal, sliding support,

$E$  – is the Young modulus, and

$J$  – is the modulus of inertia of the bent object's cross-section.

Differentiating equation (1) twice towards 'x', we subsequently obtain:

$$y'''(x) = \frac{P_1y'(x) - S_1}{EJ}$$

and  $y''(x) = \frac{P_1y''(x)}{EJ} \quad (1.a)$

where:  $y(x) = y_0(x) + y_1(x)$

Equation (1.a) finally takes the shape:

$$y''''(x) + k_1^2 y''(x) = 0$$

where:  $k_1^2 = \frac{P_1}{EJ}$

The general integral of equation (1) may be written in the form of:

$$y(x) = C_{11} + C_{21}x + C_{31} \sin(k_1 x) + C_{41} \cos(k_1 x) \quad (2)$$

The integration constants  $C_{11}$ ,  $C_{21}$ ,  $C_{31}$ , and  $C_{41}$  we determine from the boundary conditions Equation 3.

The integration constants  $C_{11}$ ,  $C_{21}$ ,  $C_{31}$ , and  $C_{41}$  obtained from the equation system are relatively equal:

$$C_{11} = -y_0 \quad (3.a)$$

$$C_{21} = \frac{y_0}{g_i} + \frac{y_0 EJ \operatorname{tg}(g_i \sqrt{\frac{P_1}{EJ}})}{g_i^2 \sqrt{\frac{P_1}{EJ}}} \quad (3.b)$$

$$C_{31} = -\frac{y_0 EJ \sec(g_i \sqrt{\frac{P_1}{EJ}})}{g_i \sqrt{\frac{P_1}{EJ}}} \quad (3.c)$$

$C_{41} = 0$  where:

$$\sec(g_i \sqrt{\frac{P_1}{EJ}}) = \frac{1}{\cos(g_i \sqrt{\frac{P_1}{EJ}})} \quad (3.d)$$

For the condition which connects the force  $P_1$  with the deformation  $\Delta g$  in the form of an implicit function  $f(P_1, \Delta g)$ , we substitute the integration constants  $C_{11}$ ,

$C_{21}$ ,  $C_{31}$ , and  $C_{41}$  determined from equation system (3) into the condition that describes the length of the curved rod, which does not changing during processing. Finally, we obtain the following expression Equation 4.

Determining the deflection  $\Delta g$  consists in substituting each value of force  $P_1$ , considered as a parameter, into equation (4) and drawing the curves of the function (Equation 5) and

$$f(P_1, g_i) = l_p \quad (6)$$

where:  $n = 100$  is the number of parts into which the interval of the function variability (2) is divided, which is accepted using intuition by the authors as giving sufficient accuracy to the calculation. The greater the value 'n', the greater the accuracy of the calculations is, but at the same time this way significantly increases the calculation time used by the computer program.

The value of  $\Delta g$ , which is related to point 'A' (the point where the function charts cross), we read from the x-axis (Figure 5, see page 80). This is a graphical solution of the equation system (5 and 6). It should be stressed that it is impossible to obtain a point  $(g_i, P_1)$  directly from equation (4) as a great number of solutions of this equation exists. The solution of this equation may be found only graphically. The reason for this is also that a symmetrical deflection line exists and that so-called 'different' buckling shapes occur, which will be discussed in the subsequent parts of this article.

$$y(0) = -y_0 \rightarrow C_{11} + C_{41} = -y_0$$

$$y'''(g_i) = S_1 = \frac{P_1 y_0}{g_i} \rightarrow -C_{31} k_1^3 \cos(k_1 x) + C_{41} k_1^3 \sin(k_1 x) = \frac{P_1 y_0}{g_i} \quad (3)$$

$$y(g_i) = 0 \rightarrow C_{11} + C_{21} g_i + C_{31} \sin(k_1 g_i) + C_{41} \cos(k_1 g_i) = 0$$

$$y''(0) = 0 \rightarrow -C_{31} k_1^2 \sin(k_1 x) - C_{41} k_1^2 \cos(k_1 x) = 0 \rightarrow C_{41} = 0$$

$$\sum_{i=1}^n \sqrt{(C_{21} \frac{g_i}{n} + C_{31} (\sin(k_1 i \frac{g_i}{n}) - \sin(k_1 (i-1) \frac{g_i}{n})) + C_{41} (\cos(k_1 i \frac{g_i}{n}) - \cos(k_1 (i-1) \frac{g_i}{n})))^2 + (\frac{g_i}{n})^2} = l_p \quad (4)$$

$$f(P_1, g_i) = \sum_{i=1}^n \sqrt{(C_{21} \frac{g_i}{n} + C_{31} (\sin(k_1 i \frac{g_i}{n}) - \sin(k_1 (i-1) \frac{g_i}{n})) + C_{41} (\cos(k_1 i \frac{g_i}{n}) - \cos(k_1 (i-1) \frac{g_i}{n})))^2 + (\frac{g_i}{n})^2} \quad (5)$$

$$y(x) = -y_0 + (\frac{y_0}{g_i} + \frac{y_0 EJ \operatorname{tg}(g_i \sqrt{\frac{P_1}{EJ}})}{g_i^2 \sqrt{\frac{P_1}{EJ}}})x - \frac{y_0 EJ \sec(g_i \sqrt{\frac{P_1}{EJ}})}{g_i \sqrt{\frac{P_1}{EJ}}} \sin(\sqrt{\frac{P_1}{EJ}} x) \quad (7)$$

Equations 3, 4, 5 and 7.

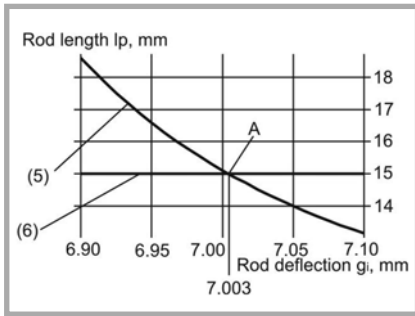


Figure 5. Determination of one of the points ( $P_1, g$ ).

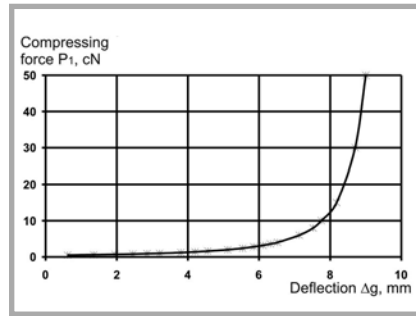


Figure 6. Mechanical characteristic  $P_1 = f(\Delta g)$  of the compressed monofilament.

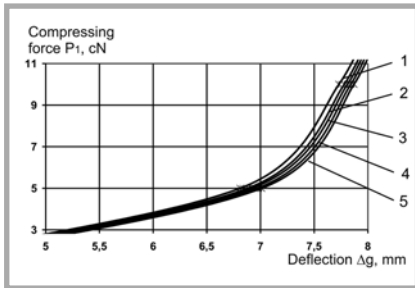


Figure 7. Dependencies  $P_1 = f(\Delta g)$  for various values of the rod's length: 1-for  $l_p = 12$  mm, 2-for  $l_p = 15$  mm, 3-for  $l_p = 20$  mm, 4-for  $l_p = 30$  mm, 5-for  $l_p = 50$  mm.

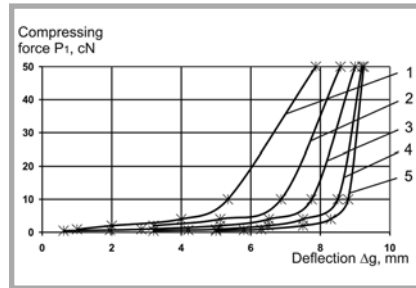


Figure 8. Dependencies  $P_1 = f(\Delta g)$  for various values of rod rigidity: 1-for  $EJ = 20,0$  cN mm<sup>2</sup>, 2-for  $EJ = 8,8$  cN mm<sup>2</sup>, 3-for  $EJ = 4,4$  cN mm<sup>2</sup>, 4-for  $EJ = 2,2$  cN mm<sup>2</sup>, 5-for  $EJ = 1,1$  cN mm<sup>2</sup>.

In this way we obtain one of the points ( $g_i, P_1$ ) of the dependency  $P_1 = f(\Delta g)$ . Irrespective of determining the dependency  $P_1 = f(\Delta g)$ , it is also possible to draw deflection lines for the bent rods by substituting the points ( $g_i, P_1$ ) obtained into the rod deflection equation (2). In this way we obtain a rod deflection equation related to the point ( $g_i, P_1$ ) in the following form (Equation 7).

The row of points ( $P_1, \Delta g = g_0 - g_i$ ) determined in the above-described way consists of the mechanical characteristic  $P_1 = f(\Delta g)$  of the compressed monofilament (Figure 6).

The mechanical characteristic was calculated and drawn for the following parameter values: knitted fabric thickness  $g = 10$  mm, rod rigidity  $EJ = 4.4$  cNmm<sup>2</sup>, rod length  $l_p = 15$  mm, mutual displacement of the monofilament fastenings in the planes of the knitted fabric  $y_0 = 2$  mm. The curve has a strongly non-linear character with a large increase in the bending force  $P_1$  at the greatest rod deflections. The mechanical characteristic  $P_1 = f(\Delta g)$  has a similar character to the one obtained empirically [10]. Notwithstanding that the mathematical analysis carried out by us concerns a single monofilament, and thanks to the assumptions for the physical model

accepted, we can obtain a general characteristic of the whole spatial knitted fabric. The force compressing the whole knitted fabric should only be divided by the number of existing connectors, and for the force thus obtained, the mechanical characteristic  $P_1 = f(\Delta g)$  would be designed. Data from comparable results attained by the mathematical simulation and by experimental tests obtained with the use of a measuring stand specially designed by us are not included in this article, as the stand is actually used later in the investigation; however they will be the subject of the next publication.

For our simulation we accepted that the thickness of the compressed knitted fabric would be  $g_0 = 10$  mm, and the rod-connector would consist of a polyamide monofilament (JPA) of  $d = 0.14$  mm. The tensile elasticity modulus was assessed empirically with the use of tensile tester from Hounsfield. The value of the Young modulus characterises the material of the rod tested. An increase in the Young modulus makes material more rigid, which means that it is not so susceptible to deformation, whereas a decrease in rod (polyamide monofilament) diameter results in an increase in the modulus of inertia  $J$  of the cross-section of the bent object, and consequently an increase in rod rigidity.

## Simulations of the compression process on the basis of the mathematical model

Aiming at the simulation of the compression process of a monofilament placed in the internal layer of a spatial knitted fabric, two calculation algorithms were elaborated, one for calculating the compression characteristic  $P_1 = f(\Delta g)$ , and the second for determining the curves representing the shape of the compressed rod. The calculations were carried out with the use of the MathCad computer program. As a result of the computer simulation, the deflection dependencies were determined as a function of the rod length  $l_p$  and rod rigidity  $EJ$ , illustrating the influence of these parameters on the values of forces and deflections (Figures 7 and 8). Figure 9 presents the curves  $P_1 = f(\Delta g)$  for different values of the rod length. Only small differences are visible in the shape of the particular dependencies. This results from the fact that the functions representing the deflection lines of the rod in the model described have a similar shape, notwithstanding relatively great differences in the lengths (significantly, the curvatures of the deflections do not mutually differ).

The examples shown in Figure 7 indicate that for various lengths  $l_p$  and for the same value of the force  $P_1$  different deflections  $\Delta g$  occur, or the opposite, formulated for the same deflection  $\Delta g$  different forces  $P_1$  is also indicated. For example, if the deflection of a rod of length  $l_p = 12.5$  mm equals  $\Delta g = 7.5$  mm, then the bending force is  $P_1 \cong 7.72$  cN, whereas for a rod of length  $l_p = 50$  mm the force is  $P_1 \cong 6,71$  cN. Thus we can conclude that the mutual relations between the force and deflection depend on the length of the rod.

On the other hand, Figure 8 presents the dependencies  $P_1 = f(\Delta g)$  for various rigidity values  $EJ$ . In this figure it is clearly visible that for various rigidities  $EJ$  of the rod and the same force  $P_1$ , different deflections  $\Delta g$  occur, or in the opposite case, for the same deflection  $\Delta g$ , different forces  $P_1$  are indicated. For example, if for a rod with a rigidity of  $EJ = 1.1$  cNmm<sup>2</sup> the deflection equals  $\Delta g = 7$ mm, then the bending force is  $P_1 \cong 1.2$  cN, whereas for a rod with a rigidity of  $EJ = 20$  cNmm<sup>2</sup>, the bending force will be  $P_1 \cong 1.2$  cN. Thus means that the rigidity of the rod increases nearly 18 times, causing the resistance to mechanical loading or load capacity of the rod to increase 30 times.

Thanks to the analysis carried out, it is visible that changes in the rigidity of the rod-connector have an significant influence on the character of the dependencies  $P_1 = f(\Delta g)$ , as they cause a low number of changes in the shape of the dependencies; a significant displacement to the left of the chart results in the same forces  $P_1$  causing a much smaller deflection  $\Delta g$ .

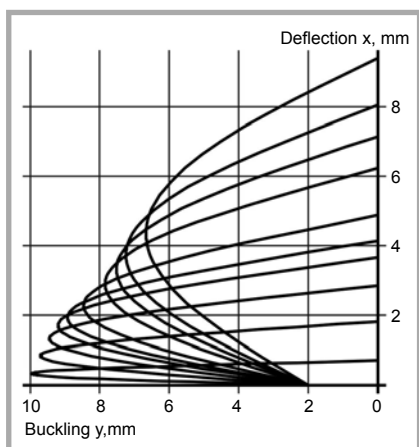


**Figure 9.** Simulation of the rod's deflection lines under the impact of force  $P_1$ , obtained using the mathematical program.

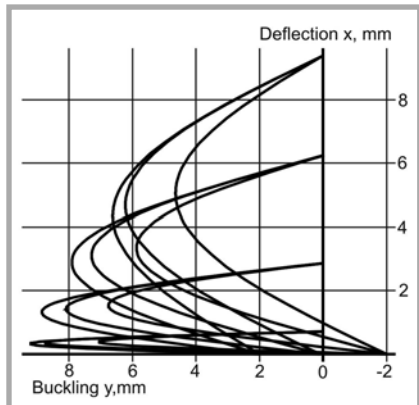


**Figure 10.** Families of curves representing the shape of monofilaments with the same deflections  $\Delta g$ , and differentiated by parameter  $y_0$ .

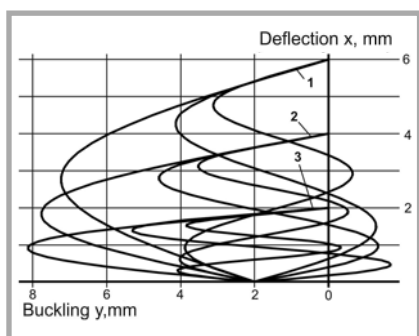


**Figure 11.** Different shapes of rod deflection caused by the action of force  $P_1$ .

A simulation of the shape of monofilaments consisting of 3D knitted fabric, which are under the influence of the compression force  $P_1$ , was also carried out. The first of the simulations performed illustrates the shape of a monofilament under the influence of force  $P_1$ .

From observation of the connector's geometry, as well as the mathematical analysis performed, it can be concluded that the rod representing the monofilament takes the shape of a fragment of a sinusoid. The shape of this sine curve depends on the value of the force  $P_1$ . With an increase in the force value, an increase in the amplitude of the curve also occurs, but it tends to be narrower. The cause of  $P_1$  increasing is, from a physical point of view, a decrease in the curvature radius of the sinusoid's apex. **Figure 9** presents a broad spectrum of deflections caused by the action of force  $P_1$ .

The next simulation was carried out with the aim of finding the influence of the distance knitted fabric's geometry on the value of the compression force  $P_1$ . It is important here to determine the influence of this force on the mutual displacement of the connector's (monofilament's) ends in the direction of the y-axis (parameter  $y_0$  is designated in **Figure 4**). Parameter  $y_0$  has three different values:

- for the symmetrical system  $y_0 \approx 0$  mm, and
- for the asymmetrical system  $y_0 = \pm 2$  mm.

**Figure 10** presents 4 families of curves representing the shape of the monofilament with the same deflections  $\Delta g$  but differentiated by the parameter  $y_0$ .

- lines 1 – force  $P_1 = 0.5$  cN for  $y_0 = 2$  mm,  $P_1 = 0.4933$  cN for  $y_0 = 0$  mm and  $P_1 = 0.4862$  cN for  $y_0 = -2$  mm,
- lines 2 – force  $P_1 = 1.2$  cN for  $y_0 = 2$  mm,  $P_1 = 1.193$  cN for  $y_0 = 0$  mm and  $P_1 = 1.043$  cN for  $y_0 = -2$  mm,
- lines 3 – force  $P_1 = 6$  cN for  $y_0 = 2$  mm,  $P_1 = 5.327$  cN for  $y_0 = 0$  mm and  $P_1 = 4.74$  cN for  $y_0 = -2$  mm,
- lines 4 – force  $P_1 = 100$  cN for  $y_0 = 2$  mm,  $P_1 = 85.96$  cN for  $y_0 = 0$  mm and  $P_1 = 74.41$  cN for  $y_0 = -2$  mm,

The differences in the bending forces, which cause the same deflections, result from the various geometries of the rods (parameter  $y_0$ ). The rods are differentiated by shape (different functions describe the shape of the curves), and with them are connected different curvature radii

of these lines, which finally leads to the situation that different forces cause the same deflection. The differences in the force  $P_1$  values change with an increase in these values: beginning with small differences of  $P_1$ , causing deflections of  $\Delta g = 0.615$  mm, to relatively high differences in  $P_1$ , which bring about deflections of e.g.  $\Delta g = 9.287$  mm. This directly results from the dependency  $P_1 = f(\Delta g)$ ; as for greater deflections the curve is steeper. The analysis also allows to state that the greatest value of  $P_1$  related to the same deflection falls when the value of parameter  $y_0 = 2$  mm. From the point of view of geometry, this can be explained by the curvature radius of the sinusoid apex related to the shape of the connector, which reaches its smallest value at this parameter value. The smaller the curvature radius of the bent rod fragment, the higher the bending tensions are in this fragment. On the other hand, the force values, which cause this deflection, depend only on the value of this spectacular (smallest) curvature radius.

The third simulation concerns the influence of the monofilament's shape on the force compressing it. This is a problem of the so-called buckling form that takes place. This phenomenon consists in them that at equal deflections  $\Delta g$  of the same rod with the same geometry of end fastenings some different values of force  $P_1$  may be created.

**Figure 11** presents the following different forms of rod deflection created by the impact of force  $P_1$ :

- 1-3 lines of the rod deflection under the impact of bending force  $P_1$  with values of  $-1.315$  cN,  $5.25$  cN, and  $11.79$  cN, causing deflections  $\Delta g$  of  $4$  mm;
- 2-3 lines of the rod deflection under the impact of bending force  $P_1$  with values of  $-3.065$  cN,  $12.25$  cN, and  $27.6$  cN, causing deflections  $\Delta g$  of  $6$  mm;
- 3-3 lines of the rod deflection under impact of bending force  $P_1$  with values of  $-12.7$  cN,  $50.07$  cN, and  $116$  cN, causing deflections  $\Delta g$  of  $8$  mm.

From observation of the connector's geometry, as well as from the mathematical analysis, it can be concluded the force causing a deflection in the case of the first buckling form is more than four times smaller than that in the case of the second buckling form, and eight times smaller than for the third case.

The practical application importance of the above-described simulation results from the fact that the rod-connector, being an element of the knitted fabric, is not isolated. The neighbouring connectors interact by contact, and the greater their number in the given volume of the knitted fabric, the greater the probability of such interaction is. Also the increase in deflection  $\Delta g$  causes a decrease in the volume of compressed rods. This, in turn, led to the mentioned increase in the probability of interaction between neighbouring monofilaments. Contact between neighbouring monofilaments causes the occurrence of higher forms of buckling, and this, in turn, increases the value of the compression force  $P_1$ , causing the same deflection  $\Delta g$ . From the curves in **Figure 11**, it is visible that the trajectories related to equal deflections  $\Delta g$  are mutually tangential, whereas the beginnings origins of the trajectories are tangential only for odd or even numbers.

## Summary

This article presents a physical and mathematical model of the process of compressing an elastic, slender rod of assumed shape fastened both sides by articulated joints. The model presented is related to the process of compressing a 3D distance knitted fabric, which we consider as a spatial trust.

1. The physical (mathematical) model is based on the following assumptions: the knitted fabric planes  $p_1$  and  $p_2$  are displaced in a perpendicular direction without deformation, the connectors are considered as elastic rods with a structure of spatial configuration, and there are elements fastening both of the sides to the outside planes of the knitted fabric by articulated joints. On the basis of the physical model, a mathematical model was developed which is a differential normal equation of the 4<sup>th</sup> order. The solution of this equation at fulfilled boundary conditions and the length condition of the rod ( $l_p = \text{constant}$ ) is the deflection line of the compressed rod. The boundary conditions (integration coefficients  $C_{12}$ ,  $C_{21}$ ,  $C_{31}$ , and  $C_{41}$ ) determine the physical (mathematical) model accepted. As a result of the mathematical analysis carried out, we obtained the following two equations:
  - an equation determining the set of points comprising the mechanical

characteristic of the compressed rod, and

- an equation determining the shape of the compressed rod.
2. A computer simulation was carried out of the compression process of a model connector of the knitted fabric which included:
    - elaboration of the mechanical characteristic of the compressed monofilament  $P_1 = f(\Delta g)$ ,
    - simulation of the influence of rod length  $l_p$ , and such structural parameters as rigidity  $EJ$ , the system's characteristic,
    - the influence of the fastening geometry of a singular monofilament on the value of force  $P_1$ , causing the monofilament's deformation,
    - Influence of different forms of buckling of the compressed monofilament which may occur on the value of deflection  $\Delta g$  at the impact of compression force  $P_1$ .

The simulation carried out demonstrated that:

- The mechanical characteristic obtained is a strong non-linear curve; at this stage of the investigation we did not find a mathematical equation of this curve which would connect the parameters of the system together.
- The change in parameter  $l_p$  causes small changes in the mechanical characteristic  $P_1 = f(\Delta g)$ ; for example, for the compression force  $P_1 = 5$  cN, the deflection difference  $\Delta g$  between the lengths  $l_p = 50$  mm and  $l_p = 12.5$  mm amounts to 0.2 mm.
- A change in the parameter  $EJ$  causes great changes in the mechanical characteristic  $P_1 = f(\Delta g)$ ; for example, for the compression force  $P_1 = 5$  cN between rigidities  $EJ = 20$  cN and  $EJ = 1.1$  cN, the deflection changes from  $\Delta g = 5.7$  mm to  $\Delta g = 1.6$  mm, respectively.
- A change in the parameter  $y_0$  (mutual displacement of the connector's fastening) influences the value of force  $P_1$ , e.g. from 3% of the  $P_1$  value for a deflection  $\Delta g = 0.6$  mm to 34% of  $P_1$  for  $\Delta g = 9.3$  mm.
- For the third form of the buckling of the bent rod, the force  $P_1$  is more than 200% greater in comparison with its value for the second buckling form, and more than 800% greater than for the first form for the same deflection  $\Delta g$  (these values differ slightly for different deflection values).

## Conclusions

The investigations carried out should be treated as an introduction to further research aimed at determining an optimum calculation model for 3D distance knitted fabrics. This involves determining the mechanical properties of such knitted fabrics, but firstly their susceptibility or resistance to compressing must be evaluated. In further parts of our research, we will design and build an empirical testing model with the aim of verifying the correctness of the mathematical models already elaborated, as well as future, new models. The next stage will be the adaptation of the calculation mechanism developed to solve real problems occurring while designing 3D distance knitted fabrics., e.g. a case of spherical loading will also be considered.

This investigation carried out by us and presented herein of an element of 3D knitted fabric in the form of a single connector, which means the elaboration of the mechanical characteristic of the compression process for this connector and the determination of its shape will be the basis for further research – more general and dedicated to designing 3D distance knitted fabrics

## References

1. K. Kopias, „Technologia dzianin kolumbijskich”, ed. WNT, Warszawa 1986.
2. W. Żurek, K. Kopias, „Struktura płaskich wyrobów włókienniczych”, ed. WNT, Warszawa 1983.
3. M. E. Niezgodziński, T. Niezgodziński, „Wytrzymałość materiałów”, ed. PWN, Warszawa 2000.
4. J. Misiak, „Stateczność konstrukcji prętowych”, ed. PWN, Warszawa 1990.
5. A. Bodnar, „Wytrzymałość materiałów”, ed. By Technical University of Krakow, Kraków 2004.
6. R. Mosurski, „Mathematica”, ed. University Scientific Editors, Kraków 2001.
7. J. Misiak, „Obliczenia konstrukcji prętowych”, ed. PWN, Warszawa 1993.
8. A. Biegus, „Nośność graniczna stalowych konstrukcji prętowych”, ed. PWN, Warszawa-Wrocław 1997.
9. W. Korliński, „Technologia dzianin rządkowych”, ed. WNT, Warszawa 1989.
10. J. Grabowski, „Dzianiny odległościowe w materacach”, *Przegląd – WOS* 10/2006.

Received 20.08.2007 Reviewed 30.10.2007